

Interaction of Ethyl Alcohol Vapor with Sulfuric Acid Solutions[†]

Raimo S. Timonen and Ming-Taun Leu*

Earth and Space Sciences Division, Jet Propulsion Laboratory, California Institute of Technology, Pasadena, California 91109

Received: October 11, 2005; In Final Form: January 24, 2006

We investigated the uptake of ethyl alcohol (ethanol) vapor by sulfuric acid solutions over the range ~40 to ~80 wt % H₂SO₄ and temperatures of 193–273 K. Laboratory studies used a fast flow-tube reactor coupled to an electron-impact ionization mass spectrometer for detection of ethanol and reaction products. The uptake coefficients (γ) were measured and found to vary from 0.019 to 0.072, depending upon the acid composition and temperature. At concentrations greater than ~70 wt % and in dilute solutions colder than 220 K, the γ values approached ~0.07. We also determined the effective solubility constant of ethanol in ~40 wt % H₂SO₄ in the temperature range 203–223 K. The potential implications to the budget of ethanol in the global troposphere are briefly discussed.

Introduction

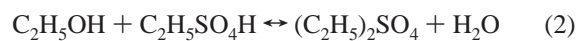
Gas-phase oxygenated hydrocarbons, particularly acetone and methanol, play an important role in atmospheric chemistry by contributing to the production of HO_x free radicals and consequently increasing the formation of ozone in the upper troposphere.^{1–8} Although ethanol is considered to be of secondary importance in these processes because its atmospheric concentrations (in the range of 20–160 ppt at 5–10 km) have been found to be smaller than those of acetone and methanol,^{1,2} it is still intriguing to investigate the production and loss mechanisms of ethanol in the global troposphere.

Sources of ethanol in the atmosphere include secondary reactions of hydrocarbons, biomass burning, and direct biogenic and anthropogenic emissions.¹ There are several loss mechanisms for ethanol. The photolytic loss of ethanol is believed to be insignificant because the photodissociation cross section in the ultraviolet region is relatively small.⁹ The solubility of ethanol in water has been reported to be about 190 mol L⁻¹ atm⁻¹ at 298 K, and the temperature dependence of $-\Delta H/R$ is 6300 (K).^{10,11} Because the solvation of ethanol in water is a reversible process, it should not be considered as a sink. It is thought that the only significant loss mechanism for ethanol in the upper troposphere is the reaction with hydroxyl radicals, because this reaction proceeds with a rather high rate of $\sim 3.2 \times 10^{-12}$ cm³ s⁻¹ at 298 K.¹²

Sulfate aerosols are thought to be the dominant form of aerosol in the lower stratosphere and upper troposphere. Very recently organic acids have been identified in situ in sulfate aerosols at an altitude of 5–19 km.¹³ These organic-containing aerosols are particularly more pronounced in the tropics because of convection in the troposphere. It is therefore intriguing to understand their formation mechanisms, such as the interaction of gas-phase organic compounds with liquid sulfuric acid.

The interaction of ethanol vapor with sulfuric acid may include mass accommodation (α), solubility (H), diffusion (D_l), reaction (k_i), and surface reaction (k_s). The uptake coefficient can be obtained by solving a set of differential equations that

incorporates the above-mentioned processes.¹⁴ To simplify the procedure, a resistor model was recently developed and has had some success.¹⁵ Typically, the accommodation coefficient, α , in H₂SO₄ is assumed to be near unity.¹⁶ The liquid-phase diffusion coefficient (D_l) can be estimated empirically with reasonable accuracy.¹⁷ The liquid-phase reactions



were investigated in the temperature range 273–298 K and acid composition 69.7–92.9 wt %.^{18–22} The forward (esterification) and backward (hydration) rates and the equilibrium constants (K) of reactions 1 and 2 were measured. The results suggest that the rates increase with acid composition and decrease with temperature. The effective Henry's law solubility constant (H^*) and surface reaction kinetics were not reported in the literature.

The reaction between ethanol with H₂SO₄ was thought to follow the esterification reaction 1. However, recent work by the Roberts group²³ on the absorption of ethanol on the concentrated H₂SO₄ (0.95 mole fraction) surface suggests that the dehydration product, C₂H₄, desorbs at the onset of H₂SO₄ sublimation. The results of a molecular beam-scattering experiment by the Nathanson group²⁴ report that the uptake coefficient on 98.8 wt % H₂SO₄ is near unity. Our investigation of the uptake processes under various conditions enables comparisons with the results of previous investigations.^{23,24}

In the upper troposphere, sulfate aerosols are mainly composed of 40–80 wt % H₂SO₄ in ambient temperatures ranging from 200 to 240 K.¹⁵ In this Article we report our investigation of the uptake coefficient and mechanisms using a fast flow-tube reactor. Our intent is to understand the possible importance of the interaction between ethanol vapor and sulfuric acid aerosol in the global troposphere. In the following sections we will discuss our experimental methods and our measurements of the uptake coefficient and its mechanisms. We will also briefly discuss the potential implications of our findings for the global atmosphere.

[†] Part of the special issue "David M. Golden Festschrift".

Experimental Methods

Apparatus. The experimental apparatus has been described in detail in previous publications.^{25,26} We used a Pyrex tubing reactor of length (l) 20 cm with an inner diameter of 1.8 cm. The bottom of the reactor was recessed to form a shallow trough of length 20 cm, 1.8 cm width, and 0.3 cm depth, which held sulfuric acid. The acid composition was varied from 40 to 80 wt %. Flowing cold methanol through the outer jacket of the reactor maintained a temperature of 193–273 K during the experiments. Humidified helium was admitted as a carrier gas through a sidearm inlet to prevent dehydration of the sulfuric acid. Ethanol vapor in another helium carrier entered the reactor through a movable Pyrex injector. Flow rates of helium carrier gas were measured by calibrated Hasting mass flow meters. A high-precision capacitance manometer (MKS Instruments, Model 390 HA) located at a downstream port monitored the total pressure in the reactor. Typically, total pressures of 0.30–0.46 Torr and flow velocities of 340–3250 cm/s inside the reactor were used. These conditions ensured that the flow was laminar and the reverse flow of ethanol vapor was minimized.

The partial pressure of ethanol used in these experiments ranged from 1.4×10^{-5} to 3.6×10^{-4} Torr, depending on the experiments performed. Ethanol vapor was monitored by the mass spectrometer at its parent peak of $m/e = 46$ amu for the selective detection sensitivity. The signal of the fragmentation peak ($m/e = 31$ amu) was stronger and was also used in some experiments for comparison with the parent peak signals.

Materials. A sample vial was temperature regulated to control the concentration of ethanol inside the reactor. Ethanol (Quantum Chemical Corp., ~100% purity) was degassed and its purity was confirmed by mass spectrometric measurements. Helium (Matheson Gas Co., 99.999% ultrahigh purity) was used as received.

Sulfuric acid solutions of known compositions were prepared by dilutions of ~96.2 wt % H₂SO₄ (J. T. Baker Chemical Co.) with distilled water. To ensure a constant composition of H₂SO₄ over a long period, the helium gas was further humidified in a vessel with H₂SO₄ of the same composition and temperature as that used in the reactor. Additionally, the acid reservoir was changed frequently, and the acid composition was checked before and after each set of experiments either by determining the density of the acid solutions as an expedient method or by titration with calibrated NaOH solutions.

Diethyl sulfates (~98% purity) were obtained from Aldrich Chemical Co. and degassed in the vacuum manifold. Diethyl sulfate was detected at its fragmentation peaks ($m/e = 99, 111, 125,$ and 139 amu) and the parent peak ($m/e = 154$ amu). Mass spectra of diethyl sulfate using the electron-impact energy of 70 V were compared with that of the NIST physical and chemical data, and both spectra were found to be in good agreement. Ethyl hydrogen sulfate was also measured at its parent peak ($m/e = 126$ amu). Unfortunately, this mass peak is very close to the fragmentation peak (125 amu) of diethyl sulfate. Thus, the identification of ethyl hydrogen sulfate is not considered to be definite.

Vapor pressures of diethyl sulfate were taken from literature.²⁷ At 320 K, the saturated vapor pressure is about 1.0 Torr. By extrapolation, at the lower temperatures used in these experiments we expect the vapor pressure to be very low. For example, the vapor pressure is about 1×10^{-5} Torr at 200 K.

We used caution when handling diethyl sulfate, because it is very sticky on both metallic and Pyrex surfaces. Because the sample decomposed rapidly in the manifold, it needed to be replaced frequently for calibration. The mass spectrometric

signals were routinely calibrated against the fresh samples to ensure the authenticity of the signals.

Liquid-Phase Diffusion Coefficient. The liquid-phase diffusion coefficient was calculated using the method previously suggested by Klassen et al.¹⁷ The diffusion coefficient of ethanol in 40–80 wt % H₂SO₄ is given by

$$D_1 = \frac{cT}{\eta} \quad (3)$$

where T is the temperature, η is the viscosity of sulfuric acid, and c is a constant determined from the molar volume of ethanol (Le Bas additivity rules). Wilke and Chang²⁸ empirically determined the value c for the species in 40–80 wt % H₂SO₄,

$$c = \frac{7.4 \times 10^{-8} (\kappa_{\text{solvent}})^{1/2}}{V_A^{0.6}} \quad (4)$$

where κ_{solvent} is a solvent-dependent empirical factor ($\kappa_{\text{solvent}} = 64$)^{28,29} and V_A is the Le Bas molar volume of solute A (ethanol) at its normal boiling temperature ($V_A = 58.37$ cm³/mol).^{28,29} We calculated c to be 5.16×10^{-8} cm² cp/(s K) for ethanol in H₂SO₄. In general, D_1 decreases with decreasing temperature and increasing acid concentration.

Uptake Coefficient Determination. The uptake coefficient was determined as follows. The loss rate of ethanol, k , was measured as a function of injector position, z , according to the following equation

$$k = -v \frac{d \ln[C]}{dz} \quad (5)$$

where C is the ethanol concentration (in units of molecules cm⁻³) and v is the average flow velocity (in units of cm s⁻¹). The reaction time was calculated by using $t = z/v$. In each experiment we calculated the cross-sectional area of the reactor and then the flow velocity. The first-order rate constant, k , was calculated from the slope of a linear least-squares fit to the experimental data.

We made a small correction due to the axial diffusion according to the equation

$$k_g = k(1 + kD_g/v^2) \quad (6)$$

where D_g is the diffusion coefficient of ethanol in He. We estimated the value $pD_g = 376$ Torr cm² s⁻¹ at 298 K, where p is the total pressure inside the reactor. A temperature dependence of $T^{1.70}$ was used for estimation of D_g at other temperatures.^{30–32} Typically, the correction for the axial diffusion is rather small, about 1–3%. We also corrected for the radial gas-phase diffusion to k_g assuming a wall-coated cylindrical reactor was used.³³ The correction is in the range 3–12%, depending upon the temperature (203–258.5 K) and k_g (~60 to ~400 s⁻¹). In general, the correction is greater at lower temperatures and larger k_g . Because of the assumption we made, the correction for radial diffusion effect is considered to be approximate.

The uptake coefficient of ethanol by sulfuric acid was determined from k_g using the equation^{25,26}

$$\gamma(t) = \frac{4k_g(V)}{\omega(S)} \quad (7)$$

where V is the volume of the reaction cell, S is the geometric area of the acid reservoir, and ω is the mean thermal speed of

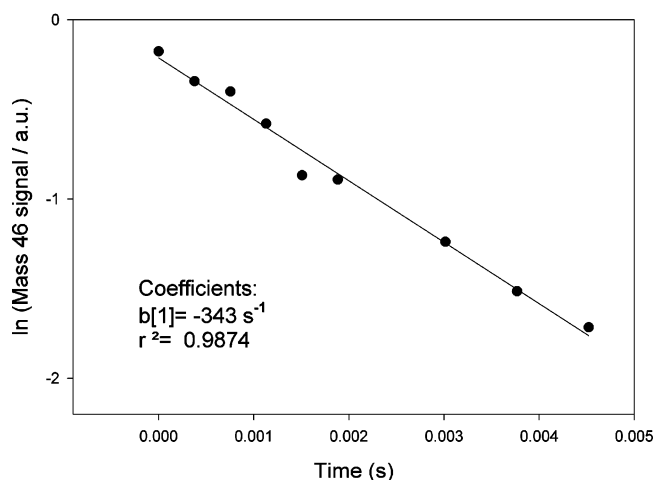
$C_2H_5OH(g) + H_2SO_4$ (70.3 wt %) at 223 K

Figure 1. Typical plot of loss of C_2H_5OH signals as a function of contact time in the interaction with H_2SO_4 . The experimental conditions are $T = 223 \text{ K}$, 70.3 wt %, $P(C_2H_5OH) = 1.9 \times 10^{-5} \text{ Torr}$, and $v = 2660 \text{ cm/s}$.

the molecule. We determined the uptake coefficients for ethanol vapor in the range of 40–80 wt % H_2SO_4 , and between the temperatures of 193 and 273 K using this procedure.

Absorption and Desorption Measurements. The uptake mechanism of ethanol vapor in H_2SO_4 was determined by sliding the injector from downstream to upstream and vice versa. We monitored the ethanol and sulfate signals while warming the reactor rapidly to near room temperature by replacing the cold methanol liquid with water in the surrounding jacket. We then determined the ratio of desorption to absorption at each experiment. This method was discussed in great detail in a recent review article that summarized our investigations of interactions between numerous trace gas molecules and liquid H_2SO_4 .³⁴

Results and Discussion

Uptake Coefficient Measurements. Initially, we filled the reactor reservoir with ~ 5 – 10 mL of acid and chilled the reactor immediately to the desired temperature. The uptake coefficient, γ , was measured by moving the Pyrex injector inside the reactor and monitoring the ethanol signals at $m/e = 46 \text{ amu}$. A typical set of data is shown in Figure 1. The data were taken at 223 K, 70.3 wt %, $p(C_2H_5OH) = 1.9 \times 10^{-5} \text{ Torr}$, and $v = 2660 \text{ cm/s}$. The observation time at each injector position was about a few seconds and the time required to complete the experiment shown in Figure 1 was $\sim 100 \text{ s}$. The ethanol signals were found to disappear linearly in the plot of $\ln[C]$ versus contact time according to eq 5. We obtained the first-order decay rate, $k = 340 \text{ s}^{-1}$, from the slope by using a linear regression method. After correcting for the effects of axial and radial diffusions, we determined the uptake coefficient to be 0.072 using eq 7.

Another set of data uses the initial ethanol pressures of (a) $1.9 \times 10^{-5} \text{ Torr}$ and (b) $4.2 \times 10^{-5} \text{ Torr}$, respectively, in the consequent experiment of $T = 203 \text{ K}$ and 54.4 wt %. Again, the ethanol signals disappear linearly, similar to the results shown in Figure 1. The uptake coefficients determined from (a) and (b) are almost identical, $\gamma = 0.069$.

The measurements of uptake coefficient are summarized in Table 1 and Figure 2. The experiments were performed in the temperature range 203–258 K and acid compositions of 41.1–79.3 wt %. As shown in the upper panel of Figure 2, in more

TABLE 1: Summary of γ Measurements for the Uptake of $C_2H_5OH(g)$ in Sulfuric Acid

H_2SO_4 (wt %)	T (K)	γ	γ (after corrections for axial and radial diffusions)	no. of experiments ^a
41.1	203	0.063	0.071(0.012) ^b	3
	213	0.060	0.067(0.028)	4
	223	0.029	0.031(0.009)	2
	233	0.018	0.019(0.002)	3
54.4	203	0.062	0.069(0.009)	4
	213	0.051	0.057(0.007)	3
	223	0.044	0.048(0.006)	4
	233	0.035	0.037(0.005)	3
64.1	243	0.032	0.033(0.005)	2
	203	0.056	0.063(0.002)	4
	213	0.056	0.062(0.007)	6
	223	0.059	0.065(0.003)	4
70.3	233	0.054	0.059(0.009)	5
	243	0.050	0.055(0.010)	4
	253	0.035	0.036(0.001)	2
	203	0.060	0.067(0.001)	2
74.4	213	0.057	0.063(0.001)	2
	223	0.065	0.072(0.001)	2
	233	0.060	0.066(0.004)	4
	243	0.052	0.057(0.001)	3
79.3	248	0.045	0.049	1
	253	0.049	0.053	1
	203	0.063	0.071(0.009)	3
	213	0.054	0.060(0.011)	3
79.3	223	0.059	0.065(0.003)	4
	233	0.050	0.055(0.008)	4
	243	0.057	0.062(0.018)	3
	248	0.044	0.048	1
79.3	253	0.058	0.063	1
	258	0.055	0.059	1
	213	0.051	0.057(0.002)	3
	223	0.060	0.067(0.002)	2
79.3	233	0.051	0.056(0.003)	7
	243	0.064	0.069	1
	248	0.056	0.061(0.007)	3
	253	0.054	0.058	1
258	0.062	0.067	1	

^a Experimental conditions: $P = 0.42$ – 0.46 Torr , $v = 2390$ – 3000 cm/s , and $P(C_2H_5OH) = (1.46$ – $5.79) \times 10^{-5} \text{ Torr}$. ^b The error limits cover the range of measurements.

concentrated solutions of 70.3–79.2 wt % the γ values appear to be nearly constant (~ 0.05 to ~ 0.07) regardless of the temperatures used in the experiment. The γ values are smaller (~ 0.02 to ~ 0.04) at warmer temperatures in more dilute solutions (see the lower panel of Figure 2).

Absorption and Desorption Measurements. To test the possible uptake mechanisms (physical or reactive) responsible for the uptake process, we performed a series of absorption/desorption experiments under similar conditions. Initially, we filled the reactor reservoir with ~ 5 – 10 mL of acid and chilled immediately to the desired temperature. At first we moved the injector to the downstream position ($l = 0 \text{ cm}$) and then pulled the injector out to the upstream position ($l = 20 \text{ cm}$), exposing the acid to ethanol vapor. The signals of ethanol vapor decrease depending upon the acid composition and temperature. After a period of ~ 2 – 20 min , we pushed the injector back to the downstream position ($l = 0 \text{ cm}$) and then measured the desorption of ethanol vapor at low temperatures. We then shut off the ethanol flow to the reactor, and the signals dropped to the background level. In the last stage of this experiment, we warmed the solutions to 293–303 K by draining out methanol and then filling the jacket of the reactor with warm water. We then measured the desorption of ethanol signals until they reached the background level.

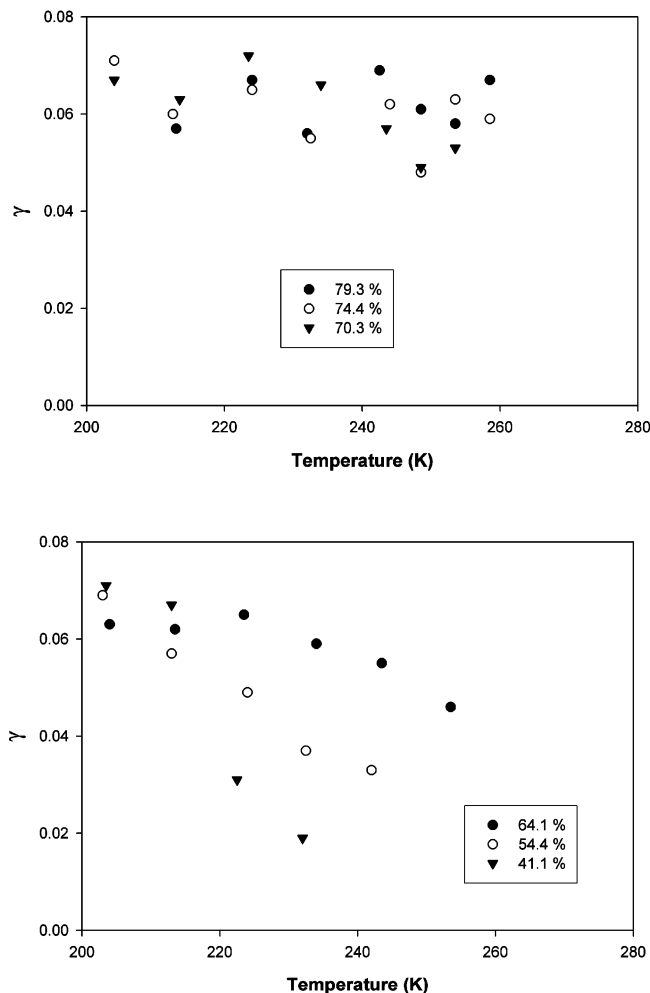
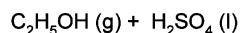


Figure 2. Dependence of uptake coefficients in the temperature range 203–258 K and concentrations of 41.1–79.3 wt %.

These experiments were taken at $T = 193\text{--}273$ K, $\text{H}_2\text{SO}_4 = 40\text{--}80$ wt %, $p(\text{total}) = 0.31\text{--}0.45$ Torr, $p(\text{C}_2\text{H}_5\text{OH}) = 1.6 \times 10^{-5}\text{--}3.5 \times 10^{-4}$ Torr, and $v = 335\text{--}2820$ cm s⁻¹. A set of the data is shown in Figure 3. We compared the absorption/desorption data at 223.5 K for three acidic solutions, (a) 41.1 wt %, (b) 70.3 wt %, and (c) 79.3 wt %. In Figure 3a the signal appears to saturate rapidly in the absorption stage because of diffusion-limited absorption/evaporation in solution. In Figure 3b,c the ethanol signals remain very low over a period of ~ 10 min because the uptake is very large. In addition, the amount of desorption at 223.5 K is more pronounced at 41.1 wt % in comparison with two other sets of data at 70.3 and 79.3 wt %. When the solution is warmed to ~ 300 K, about 10–20% of the ethanol vapor is desorbed from the liquid. Again, we note that desorption occurs immediately in the early stage of the heating ramp at a temperature of ~ 240 K. Note that the experimental conditions for Figures 1 and 3b are identical to enable useful comparison.

To estimate the effective diffusion length in these experiments (Figure 3), we used the equation $l = (\pi D_1 t)^{1/2}$.¹⁴ The diffusion coefficient (D_1) was calculated for these three cases, (a) 2.5×10^{-7} , (b) 2.3×10^{-8} , and (c) 1.7×10^{-9} (all in units of cm² s⁻¹). The diffusion length of 9.6×10^{-3} cm in (a) is longer than 6.5×10^{-3} cm in (b) and 1.8×10^{-3} cm in (c) because

Absorption and Desorption of C₂H₅OH(g) in H₂SO₄(l)

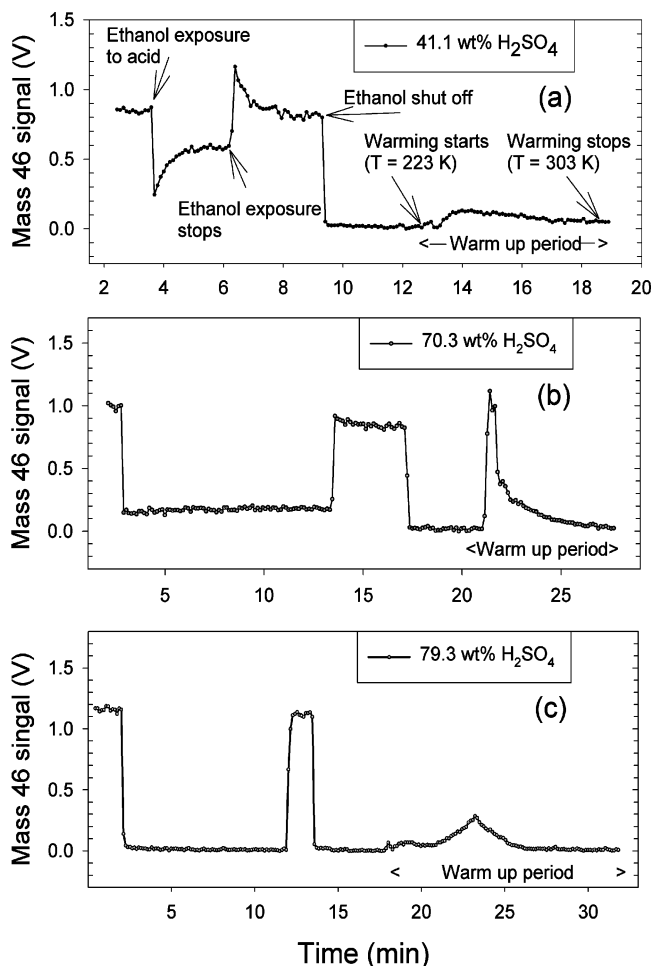


Figure 3. Absorption and desorption of C₂H₅OH in the interaction with H₂SO₄. The experimental conditions are $v = 2600$ cm/s, $T = 223$ K, and (a) 41.1 wt %, (b) 70.3 wt %, and (c) 79.3 wt %.

diffusion is much faster in dilute solutions. The calculated diffusion lengths are significantly shorter than the depth of the acid solutions (~ 0.3 cm), and hence saturation of the acidic volume by ethanol was not fully complete during the experimental runs.

The summary of the desorption-to-absorption ratio is shown in Figure 4 and also listed in Table 2. The ratio for the solutions in the range 70.3–79.3 wt % (the upper panel) is less than 10%. In more dilute solutions of 41.1–64.1 wt % (as shown in the lower panel) the ratio increases with the acid composition and temperature. This is consistent with the uptake coefficient data shown in Figure 2. Thus, the evidence suggests that the physical uptake also plays a role in dilute solutions at colder temperatures.

We also measured the ratio for desorption to absorption during the heating ramp shown in Figure 3. The ratio is about 10–40%, independent of temperature and acid composition. Because of potential complications due to reactions in the solution and desorption of diethyl sulfate during the heating period, the interpretation of this measurement is rather difficult.

Effective Henry's Law Constants at 41.1 wt % H₂SO₄.

As noted in the previous section, the uptake of ethanol vapor in solutions consists of both physical uptake and reactive uptake. Using the Resistor Model, for relatively low solubility and slow

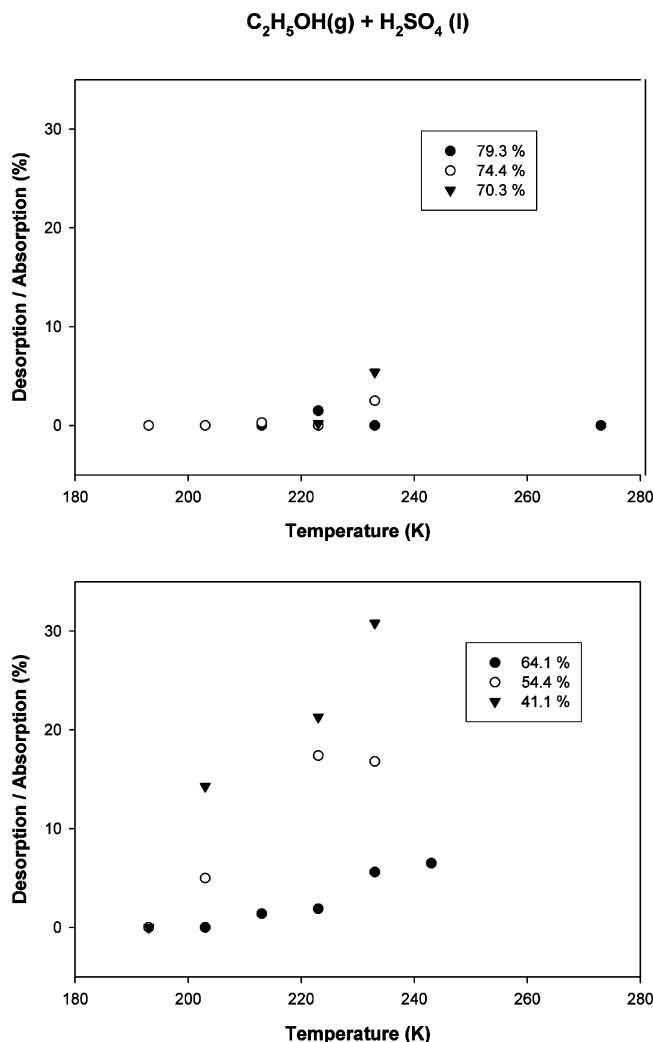


Figure 4. Ratio of desorption to absorption as a function of temperature and acid composition.

reaction times, the observed uptake coefficient, γ , can be approximately represented by^{15,34}

$$\frac{1}{\gamma(t)} = \frac{1}{\alpha} + \frac{\omega\sqrt{\pi}}{4RTH^*\sqrt{D_l}} \left(\frac{1}{\sqrt{\pi k_l} + 1/\sqrt{t}} \right) \quad (8)$$

where α is the mass accommodation coefficient, ω is the mean molecular velocity, R is the gas constant (0.082 L atm mol⁻¹ K⁻¹), T is temperature, H^* is the effective Henry's Law solubility constant, D_l is the liquid diffusion constant, and k_l is the rate constant for irreversible liquid-phase reactions. Under conditions of dilute acid compositions ($[\pi k_l t]^{1/2} \ll 1$) and low solubility, we are able to determine H^* from the plot of $1/\gamma$ versus $t^{1/2}$.

Using the absorption data (41.1 wt %) shown in Figure 3a, we calculate the uptake coefficient (γ) as a function of time for the first ~150 s. The plot of $1/\gamma$ versus $t^{1/2}$ is shown in Figure 5. The data appear to be approximately linear for the earlier contact times (<60 s), and γ remains relatively flat for later times (60–150 s). The initial slope gives a value of $H^* = 2.2 \times 10^5$ M L⁻¹ atm⁻¹.

The measurements of H^* for all data performed at 41.1 wt % H₂SO₄ are summarized in Figure 6. Our 41.1 wt % data (open circles) are very close to that of the supercooled water (filled circles) extrapolated from the data at much warmer temperatures.^{10,11} The results shown in Figure 6 are consistent with those

of acetone or methanol vapors in H₂SO₄.^{25,26,35} In both cases, the H^* at ~40 wt % H₂SO₄ are also very close to those in the supercooled water.

Because of the large uptake of ethanol signals shown in Figure 3b,c, we are not able to determine H^* in more concentrated solutions and at lower temperatures using eq 8.

Reaction Products. To identify reaction products possibly formed in the absorption/desorption experiments, we mixed 3 mL of ethanol with 10 mL of ~80 wt % H₂SO₄ inside the reactor at 296 K and then collected mass spectra repetitively by flowing helium over the solution. One set of the data is shown in Figure 7. In this spectrum there are four intense fragmentation peaks located at 99, 111, 125, and 139 amu and one weak parent peak at 154 amu. We identify it as diethyl sulfate on the basis of NIST reference data.²⁷ The 125 amu peak seems a little bit broader, which may be due to overlap with the parent peak (126 amu) of ethyl hydrogen sulfate.

In the previous section we discussed the absorption/desorption of ethanol from acidic solutions. In the same experiment we also monitored the reaction products, diethyl sulfate (the parent peak at 154 amu and the fragmentation peaks at 139, 125, 111, and 99 amu) and ethyl hydrogen sulfate (parent peak at 126 amu). One set of the data is shown in Figure 8. The experimental conditions are the same as discussed in Figure 3b. The top panel shows the temporal behavior of ethanol vapor, and the lower panel depicts that of sulfates (predominantly diethyl sulfate). When the injector was moved back to the original position ($l = 0$ cm) at ~13 min ($T = 223$ K), a very small signal of sulfate desorbed from the solution. This is not unexpected not only because the saturated vapor pressure of sulfates is very low at 223 K but also because the solution is slightly heated by the warm injector. Large sulfate signals evaporated when the reactor was heated for ~20 min ($T = 223$ K) and continuously desorbed from the solution until ~28 min ($T = 303$ K).

These experiments were also carried out under various experimental conditions. In general, the sulfate signals increase with the acid composition from ~40 to 80 wt %. This observation seems to be reasonable, because the rate of reaction 1 forming ethyl hydrogen sulfate is much greater at concentrated solutions.^{18–22} Although we observe large sulfate signals during the heating period, it should not imply that the large uptake of ethanol shown in Figures 3 and 8 at a lower temperature (223 K) is due to reactions 1 and 2 alone.

Recent work by the Roberts group²³ suggests that C₂H₄ desorbs from the surface of 0.95 mole fraction H₂SO₄ after interaction with ethanol vapor. Because the large background at 28 amu is possibly due to the presence of nitrogen or carbon monoxide in the mass spectrometer chamber, we are unable to confirm that C₂H₄ is the primary reaction product.

Comparison with the Uptake of Methanol in 40–85 wt % H₂SO₄. The absorption/desorption of methanol results are also similar to that of the ethanol uptake. At the acid compositions of 65–85 wt %, the absorption is very large and the signals remain low near background values when the injector was pulled out from downstream location (Figure 1 of ref 26). Therefore, we are unable to determine the effective Henry's law constant under this condition. Kane and Leu²⁶ assume that the uptake is entirely due to the liquid-phase reactions in concentrated acid solutions of 65–85 wt % and adopt the solubility of methanol in water in their calculation. This results in overall liquid-phase rates several orders of magnitude greater than the esterification rates reported by Deno and Newman,¹⁹ Vinnik et al.,²² and Clark and Williams.²⁰ On the basis of our ethanol uptake findings,

TABLE 2: Ratio (%) of Desorption to Absorption of C₂H₅OH in Sulfuric Acid

T (K)	H ₂ SO ₄ (wt %)					
	41.1	54.4	64.1	70.3	74.4	79.3
193	0 (4) ^a	0			0	0
203	14.3	5.0	0		0	
213			1.4 ± 0.3 (2)		0.3 ± 0.4 ^b (4)	0
223	21.3 ± 10.3 (3)	17.4 ± 2.7 (2)	1.9 ± 1.9 (3)	0.2	0 (3)	1.5 ± 1.5 (2)
233	30.8	16.8	5.6 ± 2.1 (5)	5.4	2.5 ± 3.5 (3)	0 (3)
243			6.5 ± 1.3 (2)			
273						0

^a The numbers of experiments are given in the parentheses. ^b The error limits cover the range of measurements.

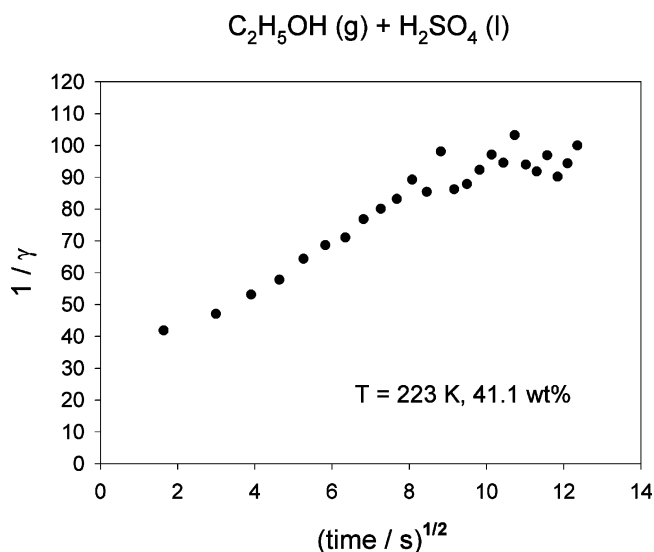


Figure 5. Plot of $1/\gamma$ vs $t^{1/2}$ for the data shown in Figure 3s. The experimental conditions are 41.1 wt % and $T = 223$ K.

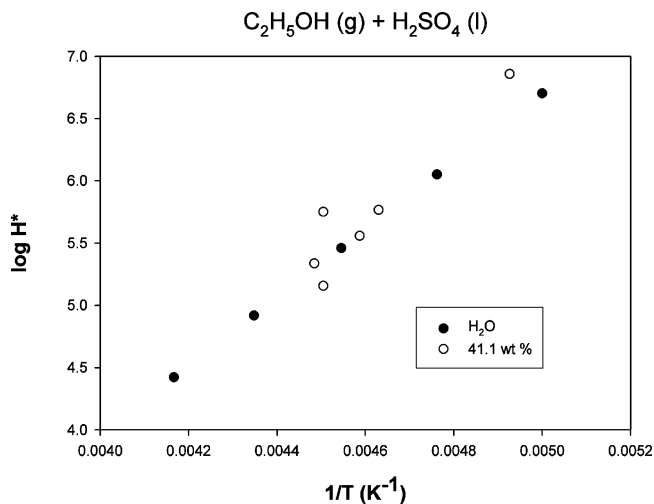


Figure 6. Plot of $\log H^*$ vs $1/T$ for supercooled water and 41.1 wt % H₂SO₄ in the temperature range 200–250 K.

we now believe both physical and reactive uptakes may be responsible for large absorption at 65–85 wt %.

The esterification rates previously determined by Clark and Williams,²⁰ Deno and Newman,¹⁹ and Vinnik et al.²² were obtained in experiments using a very large concentration of ethanol (0.1 M or greater). It is possible that their reaction rates and mechanisms may have been substantially different from the present experimental conditions using a trace of ethanol vapor absorbing, diffusing, and reacting in the condensed phase. For example, laboratory studies on the uptake of ClONO₂ molecules by sulfuric acid solutions using various reactant concentrations have shown that secondary reactions play an important role in

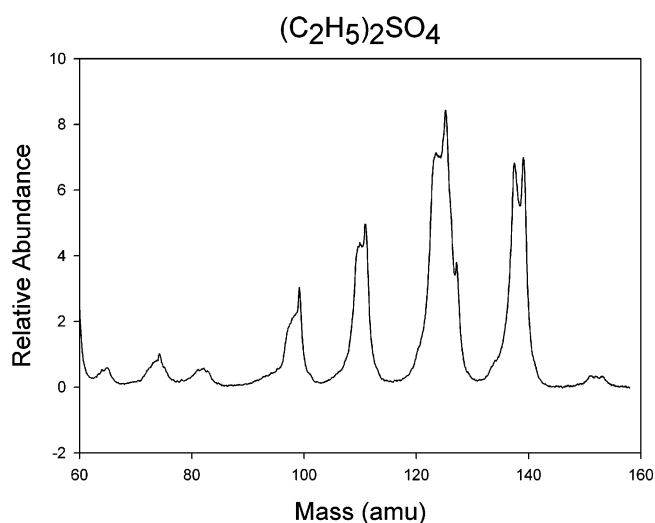


Figure 7. Mass spectrum taken from the vapor by mixing liquid ethanol and ~80 wt % H₂SO₄ in the reactor at 296 K. The mass spectrum is identified as diethyl sulfate according to the NIST physical and chemical data.

the formation of substantially different concentrations of gas-phase products, HOCl and Cl₂O.¹²

Recent work by Iraci et al.³⁵ determined the effective solubility constant of methanol in dilute solutions and further suggested that the reactive uptake is very slow, $\sim 1 \times 10^{-10} \text{ s}^{-1}$. We note that they used much larger methanol concentrations in their Knudsen cell experiments.

Atmospheric Implications. To illustrate the atmospheric importance for the uptake of ethanol in sulfuric acid aerosols, we need to discuss the loss mechanisms and their rates for typical atmospheric conditions in the upper troposphere. As noted in the Introduction, photolytic loss of ethanol is thought to be insignificant.⁵ Solubility in water droplets or uptake by ice particles in the atmosphere is also found to be very slow.^{10,11} One of the significant loss mechanisms for ethanol is the reaction with OH radicals. The estimated reaction rate for $\text{OH} + \text{C}_2\text{H}_5\text{OH} \rightarrow \text{C}_2\text{H}_5\text{O} + \text{H}_2\text{O}$ at 10 km and 220 K is calculated to be $k(\text{OH} + \text{C}_2\text{H}_5\text{OH}) \times [\text{OH}] = 7.2 \times 10^{-7} \text{ s}^{-1}$ with a lifetime of about 14 days. The rate coefficient is taken from the recommendation of the NASA Data Evaluation Panel Report,²⁸ and the diurnally averaged OH concentration is assumed to be $3 \times 10^5 \text{ molecules/cm}^3$.¹²

To calculate the loss rate of ethanol due to the uptake with sulfuric acid aerosols under tropospheric conditions (~ 220 K and ~ 40 wt %), we estimate the first-order rate using the equation, $k = \gamma\omega A/4$. The γ value (~ 0.01) is adopted from the data of 41.1 wt % H₂SO₄ at contact times of 60–150 s (Figure 5). We assume that the surface area density of sulfate aerosol at an altitude of 10 km is about $1 \times 10^{-8} \text{ cm}^2/\text{cm}^3$ under quiescent conditions, a few years after volcanic eruptions.¹² By

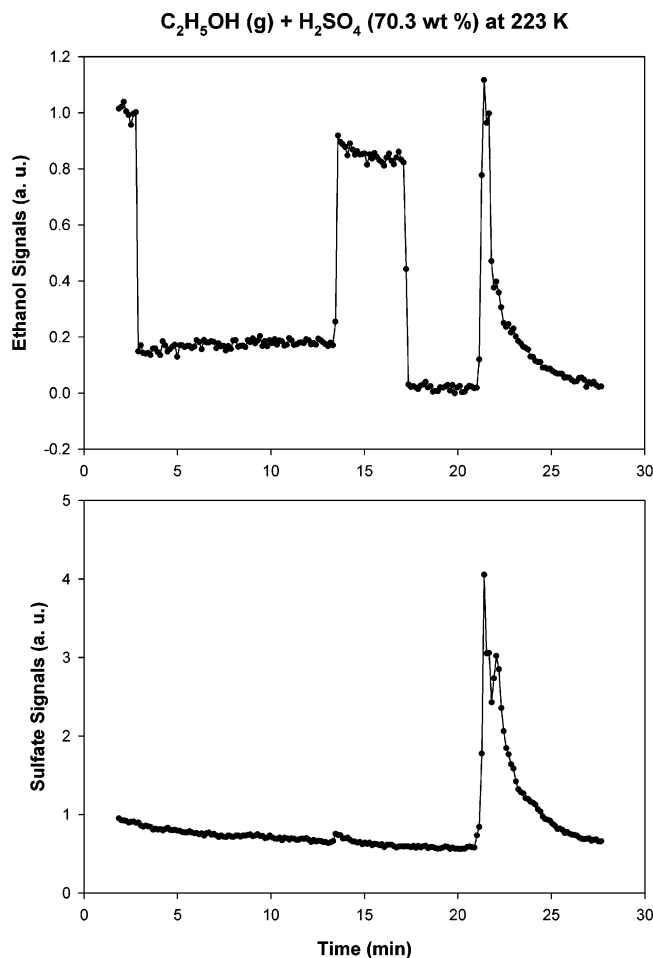


Figure 8. Desorption of ethanol (46 amu) and sulfates (parent and fragmentation peaks) during the warming process from 223 to 303 K. The baseline at the bottom panel is due to the residue in the mass spectrometer chamber. At $t = 13$ min, the sulfate signal increases slightly when the slightly warmer injector is pushed back from the upstream location. The experimental conditions are same as those in Figure 3.

using the mean thermal velocity for ethanol, ω , at 220 K, we estimate the rate to be $\sim 7.5 \times 10^{-7} \text{ s}^{-1}$. The calculation assumes that ethanol molecules are effectively removed on the surfaces of sulfuric acid aerosols and the surfaces of aerosols do not show any saturation effect under ambient conditions.

Acknowledgment. This research was performed at the Jet Propulsion Laboratory, California Institute of Technology, under

a contract with the National Aeronautics and Space Administration. R.S.T. thanks the Academy of Finland for the financial support and senior fellowship. We are grateful to Laura Iraci for helpful discussion and reviewers for useful suggestions.

References and Notes

- (1) Singh, H. B.; et al. *J. Geophys. Res.* **1994**, *99*, 1805.
- (2) Singh, H. B.; et al. *J. Geophys. Res.* **2000**, *105*, 3795.
- (3) Arnold, F.; et al. *Geophys. Res. Lett.* **1997**, *24*, 3017.
- (4) Singh, H. B.; Kanakidou, M.; Crutzen, P. J.; Jacob, D. J. *Nature* **1995**, *378*, 50.
- (5) Wennberg, P. O.; et al. *Science* **1998**, *279*, 49.
- (6) Jaegle, L.; et al. *Geophys. Res. Lett.* **1998**, *25*, 1709.
- (7) McKeen, S. A.; et al. *Geophys. Res. Lett.* **1997**, *24*, 3177.
- (8) Muller, J.-F.; Brasseur, G. *J. Geophys. Res.* **1999**, *104*, 1705.
- (9) Harrison, A. J.; Cederholm, B. J.; Terwilliger, M. A. *J. Chem. Phys.* **1959**, *30*, 355.
- (10) Snider, J. R.; Dawson, G. A. *J. Geophys. Res.* **1985**, *90*, 3797.
- (11) Betterton, E. A. *Adv. Environ. Sci. Technol.* **1992**, *24*, 1.
- (12) DeMore, W. B.; et al. JPL Publication 97-4, 1997.
- (13) Murphy, D. M.; Thomson, D. S.; Mahoney, M. J. *Science* **1998**, *282*, 1664.
- (14) Danckwerts, P. V. *Gas-Liquid Reactions*; McGraw-Hill Book Co.: New York, 1970.
- (15) Kolb, C. E.; et al. In *Progress and Problems in Atmospheric Chemistry*; Barker, J. R., Ed.; World Scientific Publication: Singapore, 1995.
- (16) Robinson, G. N.; Worsnop, D. R.; Jayne, J. T.; Kolb, C. E.; Davidovits, P. *J. Geophys. Res.* **1997**, *102*, 3583.
- (17) Klassen, J. K.; Hu, Z.; Williams, L. R. *J. Geophys. Res.* **1998**, *103*, 16197.
- (18) Deno, N. C.; Wisotsky, M. J. *J. Am. Chem. Soc.* **1963**, *85*, 1735.
- (19) Deno, N. C.; Newman, M. S. *J. Am. Chem. Soc.* **1950**, *72*, 3852.
- (20) Clark, D. J.; Williams, G. *J. Chem. Soc.* **1957**, 4218.
- (21) Williams, G.; Clark, D. J. *J. Chem. Soc.* **1956**, 1304.
- (22) Vinnik, M. I.; Kislina, I. S.; Kitaigorodskii, A. N.; Nikitaev, A. T. *B. Acad. Sci. USSR Ch.* **1986**, *35*, 2447.
- (23) Guldan, E. D.; Schindler, L. R.; Roberts, J. T. *J. Phys. Chem.* **1995**, *99*, 16059.
- (24) Fiehrer, K. M.; Nathanson, G. M. *J. Am. Chem. Soc.* **1997**, *119*, 251.
- (25) Kane, S. M.; Timonen, R. S.; Leu, M.-T. *J. Phys. Chem. A* **1999**, *103*, 9259.
- (26) Kane, S. M.; Leu, M.-T. *J. Phys. Chem. A* **2001**, *105*, 1411.
- (27) Weast, R. C.; et al. *Handbook of Chemistry and Physics*, 65th ed.; CRC Press: Boca Raton, FL, 1984.
- (28) Reid, R. C.; Prausnitz, J. M.; Poling, B. E. *The Properties of Gases and Liquids*; McGraw-Hill: New York, 1987.
- (29) Wilke, C. R.; Chang, P. *AIChE J.* **1955**, *1*, 264.
- (30) Marrero, T. R.; Mason, E. A. *J. Phys. Chem. Ref. Data* **1972**, *1*, 3.
- (31) Seager, S. L.; Geertson, L. R.; Giddings, J. C. *J. Chem. Eng. Data* **1963**, *8*, 168.
- (32) Hargrove, G. L.; Sawyer, D. T. *Anal. Chem.* **1967**, *39*, 244.
- (33) Brown, R. L. *J. Res. Natl. Bur. Stand.* **1979**, *83*, 1.
- (34) Leu, M.-T. *Int. Rev. Phys. Chem.* **2003**, *22*, 341.
- (35) Iraci, L. T.; Essin, A.; Golden, D. M. *J. Phys. Chem. A* **2002**, *106*, 4054.